Low-Cost Multi-Sensor Data Fusion for Unmanned Aircraft Navigation and Guidance

Francesco Cappello[1], Subramanian Ramasamy[2], Roberto Sabatini[3]

[1,2,3]School of Aerospace, Mechanical and Manufacturing Engineering, RMIT University, Melbourne, VIC 3000, Australia

([3]roberto.sabatini@rmit.edu.au)

Abstract- Multi-sensor navigation systems involving satellite-based and inertial sensors are widely adopted in aviation to improve the stand-alone navigation solution for a number of mission- and safety-critical applications. However such integrated Navigation and Guidance Systems (NGS) do not meet the required level of performances in all flight phases, specifically for precision approach and landing tasks. In this paper an innovative Unscented Kalman Filter (UKF) based NGS architecture for small-to-medium size Unmanned Aircraft (UA) is presented and compared with a standard Extended Kalman Filter (EKF) based design. These systems are based on a novel integration architecture exploiting state-of-the-art and low-cost sensors such as Global Navigation Satellite Systems (GNSS), Micro-Electro-Mechanical System (MEMS) based Inertial Measurement Unit (IMU) and Vision Based Navigation (VBN) sensors. A key novelty aspect of this architecture is the adoption of Aircraft Dynamics Models (ADM) to compensate for the MEMS-IMU sensor shortcomings in high-dynamics attitude determination tasks. Furthermore, the ADM measurements are pre-filtered by an UKF so as to increase the ADM validity time in the UKF based system. The improvement in Position, Velocity and Attitude (PVA) measurements is due to the accurate modeling of aircraft dynamics and integration of VBN sensors. Based on the mathematical models described, the UKF based VBN-IMU-GNSS-ADM (U-VIGA) is implemented and compared with the EKF based system (E-VIGA) in a small UA integration scheme exploring a representative cross-section of the operational flight envelope, including high dynamics manoeuvres and CAT-I to CAT-III precision approach tasks. Simulation of the U-VIGA system shows improved results when compared to E-VIGA, owing to an increase in the validity time of the ADM solution for all flight phases. The proposed NGS architectures are compatible with the Required Navigation Performance (RNP) specified in the various UA flight phases, including precision approach tasks.

Keywords-Unmanned Aircraft,Navigation and Guidance System, GNSS, Vision-based Sensors

I. INTRODUCTION

The global perspective driving Unmanned Aircraft (UA) Research and Development (R&D) is primarily aimed at addressing its integration aspects into the non-segregated airspace [16]. A number of integration solutions are being proposed and implemented to exploit the unique operational capabilities of current and future UA for a variety of research, civil and military applications. In order to fulfill the requirement of UA to routinely access and operate in all classes of airspace, a roadmap is envisaged by the International Civil Aviation Organization (ICAO) as part of Aviation System Block Upgrades (ASBU) [3]. Initial integration is envisaged by implementing basic procedures and functions including Detect-and-Avoid (DAA) functions. UA integration in traffic is foreseen by the implementation of refined procedures that would cover lost links as well as enhanced DAA functions (both cooperative and non-cooperative) with higher degree of automation and hence meeting the required level of integrity. Successively, UA transport management will involve the implementation of UA operations on the airport surface and in commercial airspace similar to conventionally piloted aircraft. Continuous airworthiness of UA is required for operating drones in unison with manned aircraft. Significant outcomes are also expected from novel Communication, Navigation, Surveillance/Air Traffic Management (CNS/ATM) systems, in line with the large-scale and regional ATM modernisation programmes including Single European Sky ATM Research (SESAR) and Next Generation Air Transportation System (NextGen). The key enabling elements required for the evolution of CNS/ATM and Avionics (CNS+A) framework have been identified as part of these programmes [5, 23]. High-integrity airborne and ground-based integrated Navigation and Guidance Systems (NGS) that include fail-safe architecture designs are required to meet the Required Navigation Performance (RNP) levels. Both Line-of-Sight (LOS) and Beyond-Line-of-Sight (BLOS) secure and safe communication links are essential for the UA to maintain continuous contact with the Ground Control Station (GCS). Enhanced surveillance solutions based on Automatic Dependent Surveillance-Broadcast (ADS-B) system and Traffic Collision Avoidance System (TCAS) are required for addressing cooperative DAA functions. The requirements for integration of UA into non-segregated airspace are outlined in Figure 1. The key contribution of the paper is on proposing enhanced navigation solutions (highlighted in Fig. 1) enabling such integration.
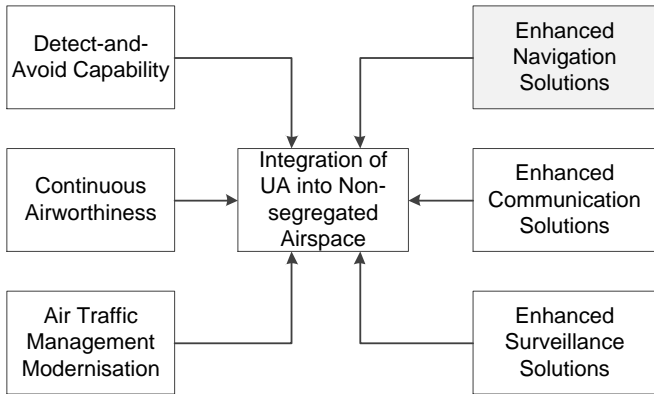
TABLE II.   Navigation Requirements for Approach Phase

RNP/ RNAV Levels	Operations in Approach Phase	Accu-racy	Alarm Limit
RNP 1	Initial/Intermediate approach	1 NM	2 NM
RNP 0.5	Initial/Intermediate/Final approach [Supports limited Category I minima]	0.5 NM	1 NM
RNP 0.3	Initial/Intermediate/Final approach [Supports limited Category I minima]	0.3 NM	0.6 NM
RNP 0.3 / 125 ft	Initial/Intermediate/Final approach with specified barometric vertical guidance [Supports limited Category I minima]	0.3 NM / 125 ft	0.6 NM / 250 ft
RNP 0.03 / 45 ft	Final approach with specified vertical guidance [Supports Category I minima]	0.03 NM / 45 ft	0.06 NM / 90 ft
RNP 0.01 / 15 ft	Final approach with specified vertical guidance [Supports Category I/II minima]	0.01 NM / 15 ft	0.02 NM / 30 ft
RNP 0.003 / 15 ft	Final approach with specified vertical guidance [Supports Category I/II/III minima]	0.003 NM / 15 ft	0.006 NM / 30 ft

Figure 1.   Requirements for integration of UA into non-segregated airspace

II.   UA NAVIGATION

In order to obtain an effective separation between manned aircraft and UA, the Performance Based Navigation (PBN) approach enforces a set of Required Navigation Performance (RNP) standards related to the different flight phases. The required RNP accuracies and alarm limits are summarised in Table 1 [10] and specific RNP values for the approach phase are shown in Table 2 [4].

TABLE I.   Navigation Requirements for Different Flight Phases

RNP/RNAV Levels	Flight Phase	Accuracy	Alarm Limit
RNAV 10	En route	10 NM	20 NM
RNAV 10	En route, arrival	5 NM	10 NM
RNAV 2	En route, arrival, departure	2 NM	4 NM
RNAV 1	En route, arrival, approach, departure	1 NM	2 NM
RNP 4	En route	4 NM	8 NM
Basic RNP 1	Arrival, approach, departure	1 NM	2 NM
RNP APCH	Final approach	0.3 NM	0.6 NM

The PBN concept specifies that aircraft RNP and area navigation (RNAV) performance requirements are defined in terms of accuracy, integrity, availability and continuity, and it is necessary to meet the accuracy levels [11]. These navigation specifications are defined at a sufficient level of detail in order to facilitate global harmonization by providing specific implementation guidance for national aviation regulators and operators. The required navigation performances are in turn translated to technical requirements, which aid in the determination of specific airborne sensors that can be employed onboard the UA. The UA sensor requirements dictate the following: physical characteristics of the sensors including size, weight and volume, support requirements such as electrical power, accuracy and precision.

The selection of the navigation sensors is based on the requirements of low-cost, low-weight/low-volume sensors capable of providing the required level of performance in all flight phases of a small-to-medium size UA including high dynamics manoeuvres. Global Navigation Satellite System (GNSS) and Micro-Electro-Mechanical System (MEMS) based Inertial Measuring Unit (IMU) are a highly synergistic combination of navigation sensors capable of providing an accurate navigation state vector. GNSS provides a more consistent Position, Velocity and Attitude (PVA) data as well as time information. Since the Inertial Navigation System (INS) measurements are only accurate for a short period of time and drift gradually, they are augmented with the GNSS estimate values. In the case of small-to-medium size UA, Micro-Electro-Mechanical System (MEMS) based IMU sensors are employed due to its low-cost and low-weight characteristics. The limiting factor of MEMS based IMU is the large sensor errors rapidly degrade the navigation performance at an exponential rate. These error coefficients can be used further in the Kalman filter for better navigation performance and in the Doppler frequency estimate for faster acquisition during an event of GNSS signal loss or outage [30]. The most crucial aspect, if one relies on an inertial system for air navigation, is the determination of correction factors for providing the Most Probable Position (MPP). The recent advances in the field of electro-optics have made Vision Based Navigation (VBN) a viable option for increasing the positional accuracy in UA applications especially for precision approach and landing [2]. Vision-based methods provide cost effective solutions and are also not subject to the same limitations as GNSS/INS sensors. Additionally, the solution provided by VBN sensors are self-contained and autonomous, which enables them to be used as an alternative to more traditional

sensors including INS and GNSS [24]. Additionally, an Aircraft Dynamics Models (ADM) is used to compensate for the VBN and MEMS-IMU sensor shortcomings experienced in high-dynamics attitude determination tasks. The ADM virtual sensor is essentially a Knowledge-Based Module (KBM), which is used to augment the navigation state vector by predicting the UA flight dynamics. The ADM employs either a three-degree-of-freedom (3-DoF) or a six-degree-of-freedom (6-DoF) variable mass model with suitable controls and constraints applied in the different phases of flight.

III. MULTI-SENSOR DATA FUSION

The multi-sensor navigation system processes the navigation sensor information and provides an estimate on PVA from a sequence of measurements provided by the sensors. The INS is prone to an accumulation of unbounded errors in the navigation variables as a function of time or distance travelled. GNSS relies on information received from off-board components and is susceptible to intentional or unintentional Radio Frequency Interference (RFI) including jamming and spoofing [24]. The ADM is prone to rapid divergence due to the accumulation of errors in the obtained PVA parameters. Hence effective data-fusion algorithms are developed to address the shortcomings. As a result of extensive research activities performed based on a number of NGS, it was observed that the image processing frontend was susceptible to false detection of the horizon if any other strong edges were present in the image [25-27]. Therefore, an Extended Kalman Filter (EKF) was implemented to filter out these incorrect results [27]. The ADM is also used to compensate for the MEMS-IMU sensor shortcomings experienced in high-dynamics attitude determination tasks. The EKF is employed for a number of applications including missile [18, 21], feature [9, 17], and vision based tracking [7, 8], data fusion/integration [27, 28], improved navigation [6, 27, 28], and robotic control [20]. The EKF operates by approximating the state distribution as a Gaussian Random Variable (GRV) and then propagating it through the first-order linearization of the nonlinear system [29]. The EKF accounts for nonlinearities by linearizing the system about its last-known best estimate with the assumption that the error incurred by neglecting the higher-order terms is small in comparison to the first-order terms [29]. The EKF is a suboptimal nonlinear filter due to the truncation of the higher-order terms when linearizing the system [29]. The drawback in adopting an EKF is the complexity involved in the derivation of the Jacobian matrices and the linear approximations of the nonlinear functions. Furthermore, the accuracy of propagated mean and covariance is limited to first order, since the filter employs a linearization method based on the first-order truncated Taylor series [14]. The original UKF was first developed by Julier et al. [22] and modified into a number of different algorithms successively. The idea behind modifying the EKF to the UKF is because recent studies have suggested that implementing the EKF gives rise to a number of performance flaws, where most deficiencies are succinctly addressed by the UKF [15]. The UKF overcomes the limitations of the EKF. Sigma-point Kalman Filters (SPKFs), such as the unscented filter, provide derivative-free higher-order approximations by approximating a Gaussian distribution rather than approximating an arbitrary nonlinear function as the EKF does. Table 3 lists the merits, demerits, resultant ADM validity time and processing mechanisms employed in the proposed NGS architectures.

TABLE III.   COMPARISON OF EXTENDED AND UNSCENTED KALMAN FILTERS

	EKF	UKF
Advantages	Reliable, proven, computationally fast and highly efficient	Derivative free (No Jacobeans needed), simple and better, better approximation of nonlinear models, better linearization than EKF, higher degree of accuracy in first two terms of Taylor expansion
Disadvantages	Use of Jacobeans, complex, less optimal, diverges if nonlinearities are high	Performance degrades with very high nonlinearities
ADM validity time	Medium	High
Processing	Main processor	Main and pre-processor

In case of navigation applications, the UKF is more robust and accurate than EKF and provides better convergence characteristics. The nonlinear transformations of sigma points (mean values) are intended to be an estimation of the posterior distribution, the moments of which can then be derived from the transformed samples. This transformation is referred to as the Unscented Transform (UT) and allows the UKF to capture first and second order terms of the nonlinear system. These sample points capture the mean and covariance accurately up to the third order and it is possible to reduce errors in the higher-order terms as well. Additionally, because no explicit Jacobian or Hessian calculations are necessary, the UKF is easier to implement.

The UKF is classified into [13]:

- Additive UKF that reduces the order and subsequently the number of mathematical calculations required in each iteration, without using the augmented states of the traditional UKF. This filter is computationally efficient and hence adopted in real-time systems.
- Square-root UKF that is used to prevent numerical instabilities to which the algorithm is exposed, being necessary to conserve the covariance matrix of the state errors as semi-defined positive.
- Spherical simplex UKF that utilizes an alternative criterion for selecting a minimum set of sigma points. This variant

overcomes a key drawback of the UKF, which is the relative poor execution speed when compared to EKF.

The UT process is based on a sequence of tasks: computation of a set of sigma points, assignment of weights to each sigma point, transformation of the sigma point through a nonlinear function and computation of the Gaussian weighted points. As depicted in Figure 2, the sigma points are obtained based on the mean and covariance values and the UT process transforms the sigma points to a new set.

Sigma Points: Blue
Mean: Black
Covariance: Red circumference
Transformed Sigma Points: Orange
Mean obtained after UT: Grey
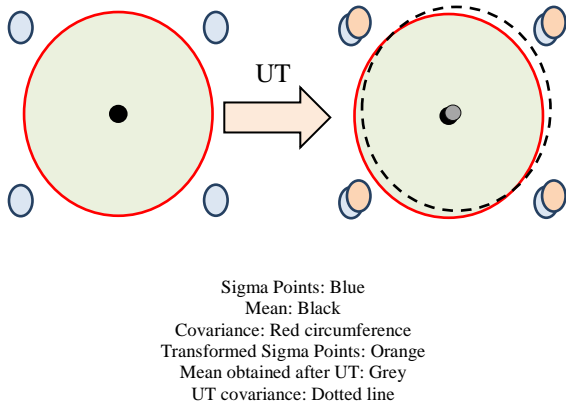UT covariance: Dotted line

Figure 2.   Sigma points and transformed sigma points

An enhanced NGS concept is developed by implementing an UKF, which specifically addresses the corrections required for navigation errors of the 6-DoF dynamics model as illustrated in Figure 3. In this low-cost NGS, the information from a number of aircraft sensors are fused into a federated UKF architecture and thus providing additional information to increase the accuracy of the state vector. Stemming from [26, 27], a number of additions have been proposed in the novel multi-sensor data fusion architecture to enhance its overall performance. The selection employs two state-of-the-art physical sensors: MEMS-based INS and GNSS. The ADM acts as a virtual sensor and also operates in parallel with the centralised UKF. The error analysis blocks assimilate information from the primary sensors and compares the errors with that of the navigation solution obtained from the virtual sensor. Additionally, the UKF is also used to pre-process the ADM navigation solution. The pre-filtering of the ADM measurements leads to an improvement of the overall PVA error budget and specifically increases the validity time of the ADM solution. The centralised UKF, also known as the master UKF, is the central component of the proposed architecture and is used to fuse the navigation sensor data to obtain the navigation solution.
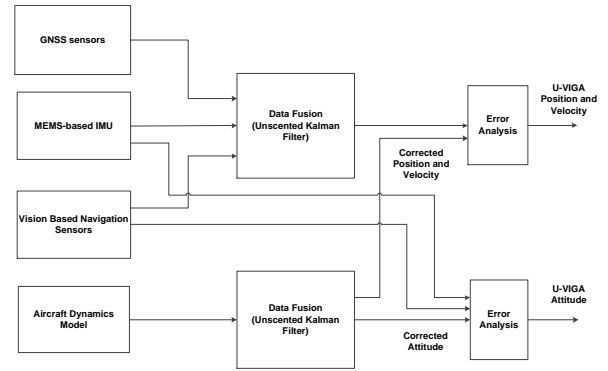

Figure 3.   UKF NGS architecture

IV.   MATHEMATICAL MODELS

The multi-sensor data fusion architecture is based on a federated architecture. The process model is based on a set of sigma points, which are selectively chosen for improving the performance of the data fusion process. The sample value equations are given below:

$$\chi_0 = x_m \tag{1}$$

$$\chi_i = x_m + \left(\sqrt{(n+\kappa)P_{xx}}\right)_i \tag{2}$$

$$\chi_i = x_m - \left(\sqrt{(n+\kappa)P_{xx}}\right)_{i-n} \tag{3}$$

where χ is the initial mean of the sigma points (sample values), P_{xx} is the initial covariance matrix, m is the mean value, i is the index value given by $i = 1,2,\dots,n$, κ is the integer scaling factor and n is the outer value. κ is introduced as a tuning parameter for the calculation of the sigma points. The algorithm is designed to sample the mean and covariance of an arbitrary function that satisfies its state variable and follows a normal distribution. The nonlinear function is applied to each sigma point, which in turn yields a cloud of transformed points and the statistics of the transformed points. Since the problem of statistical convergence is not a substantial drawback, higher order information about the distribution can be captured using only a very small number of points [19]. The UT process is described by introducing a random variable x (dimension n) and is assumed to be propagated through a nonlinear function, $f = g(x)$ and x is represented by the mean and covariance values. At the end of this process, a valid selection of sigma points is obtained. The transformed points are given a weighting known as sample weight that are given by:

$$W_i = \frac{\kappa}{n+\kappa} \tag{4}$$

$$W_{i+1} = \frac{1}{2(n+\kappa)} \tag{5}$$

$$W_{i+n+1} = \frac{1}{2(n+\kappa)} \tag{6}$$

where W is the initial weight. The sample values attained from the measurements are fed into the UKF. In the equations above $\left(\sqrt{(n+\kappa)P_{xx}}\right)_i$ is equal to u_i which is a row vector. These values are obtained from the matrix $U^T U = (n+\kappa)P_x$, where κ is an arbitrary constant. These sigma vectors are propagated through another nonlinear function $y_i = g(\chi_i)$. The mean and covariance of $y = f(x)$, are calculated using:

$$y_m = \sum_{i=1}^{2n+1} W_i f(\chi_i) \qquad (7)$$

$$P_y = \sum_{i=1}^{2n+1} W_i \{f(\chi_i) - y_m\}\{f(\chi_i) - y_m\}^T \qquad (8)$$

The weights are assumed as constant for each of the sigma points when the mean and covariance are calculated. The sigma points and weights satisfy the following equations:

$$x_m = \sum_{i=1}^{2n+1} W_i \chi_i \qquad (9)$$

$$P_x = \sum_{i=1}^{2n+1} W_i \{\chi_i - x_m\}\{\chi_i - x_m\}^T \qquad (10)$$

The sigma points and statistical properties are obtained from the state variables. The mean and covariance are obtained from the transformed result of the sigma points. The transformation process is listed below:

• The chosen sigma points χ_i are selected based on the mean and covariance of x.
• The sigma points are then transformed through the function $f(x)$.
• The weighted mean and covariance are calculated with the new sigma points $f(\chi_i)$.
• Once these steps are carried out the mean and covariance of $f(x)$ values are what remains.

Once the UT is processed, the state variable is processed through the UKF loop. The first step in the transformation process is to use the time-update equations to transform the sigma points, this step is also known as the prediction step. These updates are performed for each time step $k = 1,2\cdots,n$. The sigma points are computed as follows:

$$S_{k-1} = \{chol(P_{k-1})\}^T \qquad (11)$$

$$X_{\kappa-1} = \{\hat{x}_{\kappa-1} \; \hat{x}_{\kappa-1} + \gamma S_{\kappa-1} \; \hat{x}_{\kappa-1} - \gamma S_{\kappa-1}\} \qquad (12)$$

where P is the lower triangular matrix of the Cholesky factorisation S and γ is the control parameter of the dispersion distance from the mean estimate in the computation of the sigma point matrix X. The time-update equations, which are used to transform the sigma points, are given by:

$$X^*_{\kappa|\kappa-1} = f_d(X_{\kappa-1}, u_{k-1}) \qquad (13)$$

$$\hat{x}^-_\kappa = \sum_{i=0}^{2n} w_i X^*_{i,\kappa|\kappa-1} \qquad (14)$$

$$P^-_k = \sum_{i=0}^{2n} w_i^{(c)} \left(X^*_{i,\kappa|\kappa-1} - \hat{x}^-_\kappa\right)\left(X^*_{i,\kappa|\kappa-1} - \hat{x}^-_\kappa\right)^T \qquad (15)$$

Furthermore, once the time-update has been processed, the measurements are also updated given by:

$$\mathcal{K} = P_{x_\kappa y_\kappa} P^{-1}_{\tilde{y}_\kappa \tilde{y}_\kappa} \qquad (16)$$

$$\hat{x}_\kappa = \hat{x}^-_\kappa + \mathcal{K}(y_\kappa - \hat{y}^-_\kappa) \qquad (17)$$

$$P_\kappa = P^-_\kappa - \mathcal{K} P_{\tilde{y}_\kappa \tilde{y}_\kappa} \mathcal{K}^T \qquad (18)$$

$$P^-_\kappa = \sum_{i=0}^{2n} w_i^{(c)} \left(y^*_{i,\kappa|\kappa-1} - \hat{y}^-_\kappa\right)\left(y^*_{i,\kappa|\kappa-1} - \hat{y}^-_\kappa\right)^T \qquad (19)$$

In contrast to the EKF, it can be seen in Figure 4 that no computation of Jacobians or Hessians are in the UKF algorithm and neither are they necessary to be implemented. The UKF algorithm is used for both the master Kalman filter and the ADM. The Aerosim blockset, which is a MATLAB^{TM} and Simulink library of components for rapid development of nonlinear 3-DoF and 6-DoF aircraft dynamics models, is adopted to realise the ADM. In addition to aircraft dynamics, the blockset also includes environment models such as standard atmosphere, background wind, turbulence, and the Earth models (geoid reference, gravity and magnetic field). The position of the UA is determined by the 6-DoF geodetic nonlinear equations of motion in scalar form given by:

$$\dot{P}_N = (cos\Theta cos\Psi)u + (-cos\Phi sin\Psi + sin\Phi sin\Theta cos\Psi)v + (sin\Phi sin\Psi + cos\Phi sin\Theta cos\Psi)w \qquad (20)$$

$$\dot{P}_E = (cos\Theta sin\Psi)u + (cos\Phi cos\Psi + sin\Phi sin\Theta sin\Psi)v + (-sin\Phi sin\Psi + cos\Phi sin\Theta cos\Psi)w \qquad (21)$$

$$\dot{h} = (-sin\Theta)u + (sin\Phi cos\Theta)v + (cos\Phi cos\Theta)w \qquad (22)$$
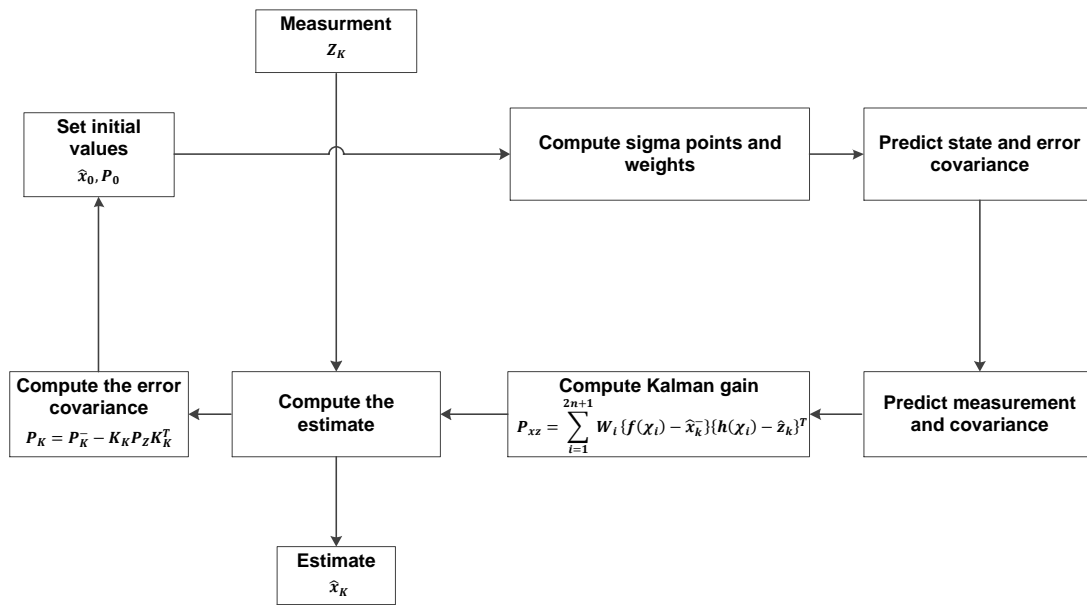
Figure 4.   UKF process

V.   NAVIGATION AND GUIDANCE SYSTEM DESIGN AND SIMULATION

A number of integrated navigation system architectures were defined as part of earlier research activities; including EKF based VBN-IMU-GNSS (E-VIG) and VBN-IMU-GNSS-ADM (E-VIGA) and VBN-IMU-GNSS-GAD (E-VIGGA) [26, 27] systems. The E-VIG architecture uses VBN at 20 Hz and GPS at 1 Hz to augment the MEMS-IMU running at 100 Hz. The E-VIGA architecture includes the ADM (computations performed at 100 Hz) to provide attitude channel augmentation whereas the E-VIGGA architecture includes GNSS to provide attitude channel augmentation. The corresponding E-VIG, E-VIGA and E-VIGGA integrated navigation modes were simulated using MATLAB[TM] covering all relevant flight phases of an AEROSONDE UA (straight climb, straight-and-level flight, level turn, climb/descend turn, straight descent, etc.). The navigation system outputs were fed to a hybrid Fuzzy-logic/PID controller designed for the AEROSONDE UA and capable of operating with stand-alone VBN, as well as with other sensors data. In the E-VIGA architecture the INS provides measurements from gyroscopes and accelerometers which are fed to a navigation processor. GNSS provides raw pseudorange measurements which are processed by a filter to obtain position and velocity data. The INS position and velocity provided by the navigation processor are compared to the GNSS data to form the measurement input of EKF. Additionally, in this case, the attitude data provided by the ADM and the INS are compared to feed the EKF at 100 Hz, and the attitude data provided by the vision based sensors and INS are compared at 20 Hz and input to the EKF. The EKF provides estimations of PVA errors, which are removed from the INS measurements to obtain the corrected PVA states. Again, the corrected PVA and estimates of accelerometer and gyroscope biases are used to update INS raw measurements. The attitude best estimate is compared with the INS attitude to obtain the corrected attitude. In the evolution of the E-VIGA architecture, the EKF is replaced with UKF as the main processor in U-VIGA and also adopted to pre-process the ADM navigation solution. The pre-filtering of the ADM virtual sensor measurements results in achieving reduction of the overall position and attitude error budget and importantly considerable reduction in the ADM re-initialisation time. PVA measurements are obtained as state vectors from both the centralised UKF and ADM/UKF and are compared in an error analysis module. The U-VIGA architecture is illustrated in Figure 5.
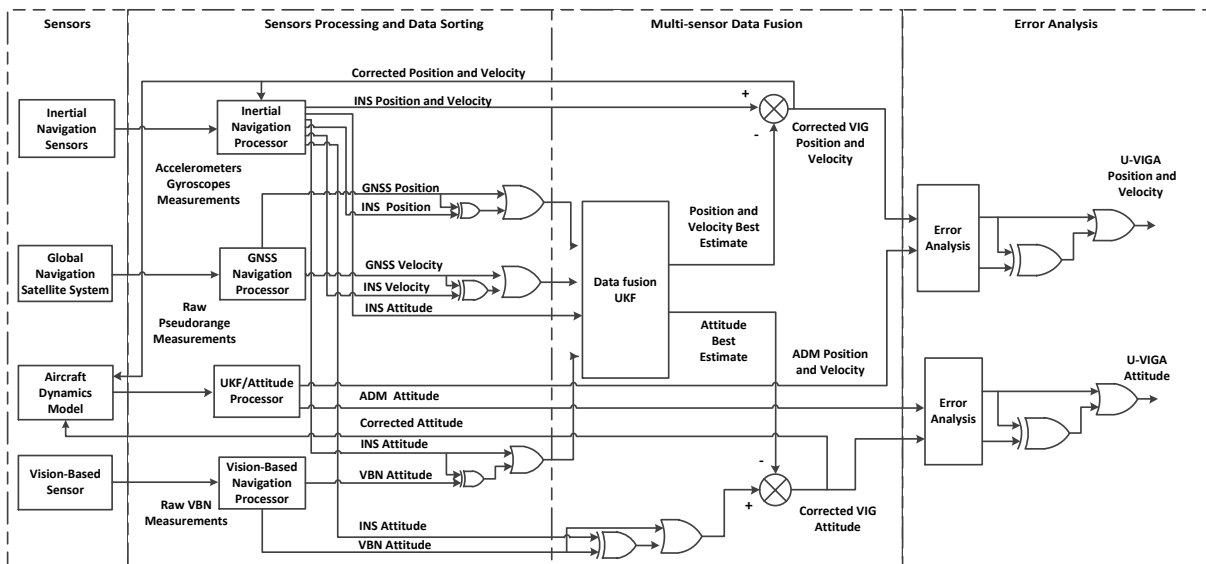
Figure 5.   U-VIGA system architecture

The E-VIGA and U-VIGA architectures were tested by simulation in an appropriate sequence of high dynamics flight manoeuvres representative of the AEROSONDE UA operational flight envelope. The duration of the simulation is 750 s. The 3D trajectory plot of the flight phases followed by the AEROSONDE UA is shown in Figure 6.
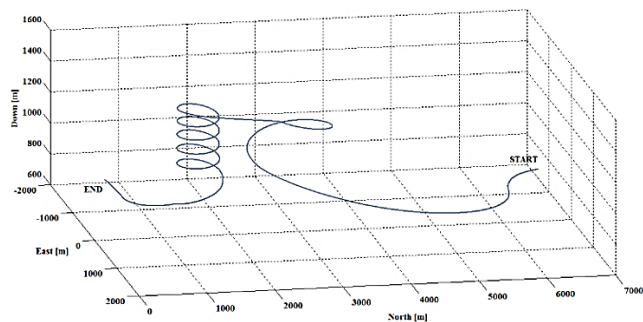

Figure 6.   3D trajectory plot of UA flight phases.

The position and attitude error time histories obtained in U-VIGA system are shown in Figure 7 and Figure 8 respectively. A comparison is made between E-VIGA and U-VIGA position and attitude errors. It is inferred that the adoption of UKF provides substantial improvement to the obtained navigation solution.
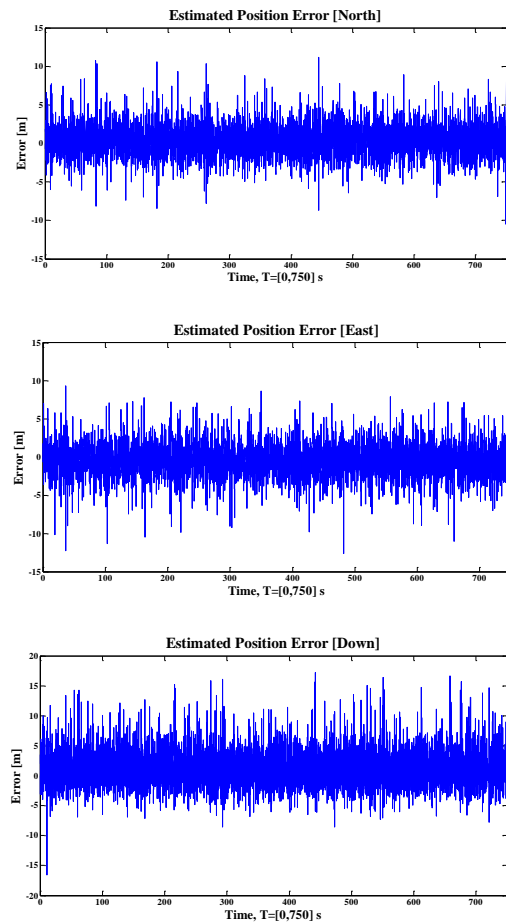

Figure 7.   U-VIGA position error time histories.

The PVA best estimates of the two NGS architectures are obtained and the associated error statistics (mean, μ and standard deviation, σ) are calculated.
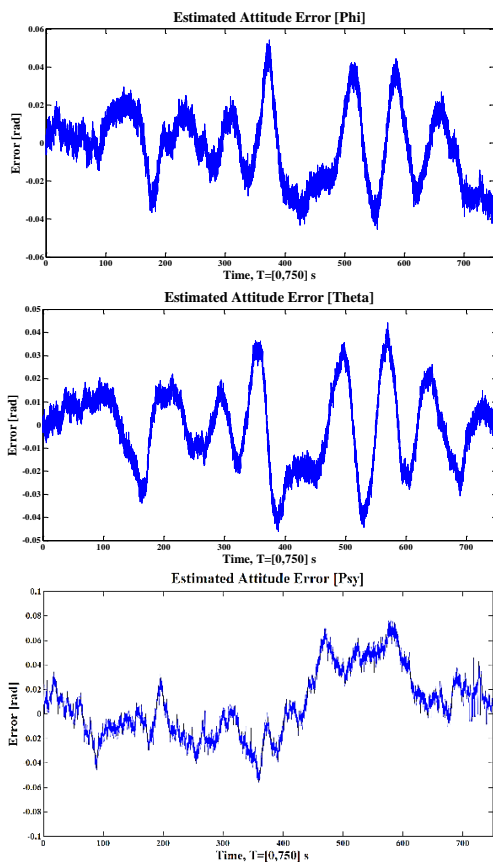

Figure 8. U-VIGA attitude error time histories.

The ADM validity times for the estimated position error are illustrated in Figure 9.
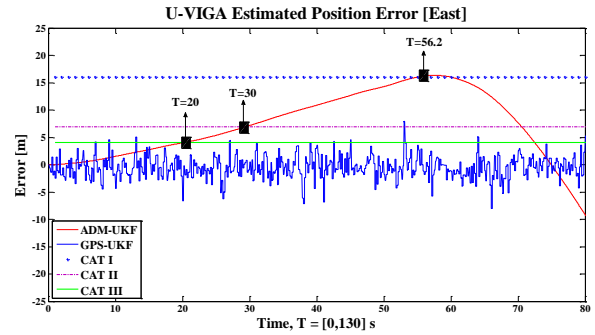

Figure 9. Comparison of ADM validity times.

The E-VIGA NGS system is prone to rapid divergence and its optimal time for re-initialisation is in the order of 20 seconds. The U-VIGA NGS system shows considerable improvement in the horizontal and vertical positions. Additionally, the U-VIGA system demonstrates promising results in the performance of the modified ADM. By applying an UKF to pre filter the ADM measurements, the navigational solution is corrected and it is useful for an extended period of operation. Comparing with the E-VIGA solution, a significant improvement of the solution validity time is obtained with the U-VIGA system. In particular, the validity time before the solution exceeds the RNP 1 threshold in the climb phase is 76 sec and, in the final approach phase, the ADM solution exceeds the CAT I, CAT II and CAT III limits at 56.2 sec, 30 sec and 20 sec respectively (the VIGA was compliant with CAT I up to 36 sec, CAT II up to 19 sec and CAT III up to sec to 16 sec). The vertical channel was found to satisfy CAT III and CAT II requirements up to 100 sec and CAT I requirements up to 365 sec. The position and attitude error statistics of the two NGS architectures are listed in Tables 4 and 5 respectively. Table 6 lists a comparison of the E-VIGA and U-VIGA position and attitude horizontal and vertical accuracy (RMS-95%) with the required accuracy levels for precision approach as recommended by the International Civil Aviation Organization [1, 12] and the obtained results are in line with CAT II precision approach requirements.

TABLE IV. POSITION ERROR STATISTICS

NGS Architecture	North Position [m]		East Position [m]		Down Position [m]	
	μ	σ	μ		μ	σ
E-VIGA	0.3652	1.9028	-0.4849	E-VIGA	0.3652	1.9028
U-VIGA	0.4793	1.4062	-0.4064	U-VIGA	0.4793	1.4062

TABLE V. ATTITUDE ERROR STATISTICS

NGS Architecture	Pitch (θ) [degrees]		Roll (φ) [degrees]		Heading (ψ) [degrees]	
	μ	σ	μ	σ	μ	σ
E-VIGA	0.0052	0.0406	-0.0065	0.3138	-0.0011	0.0447
U-VIGA	0.0051	0.0400	-0.0053	0.2197	0.0010	0.0417

TABLE VI. E-VIGA AND U-VIGA POSITION ERROR STATISTICS (PRECISION APPROACH).

Category of approach	Horizontal Accuracy (m) 2D RMS - 95%			Vertical Accuracy (m) RMS - 95% Down		
	Required	E-VIGA	U-VIGA	Required	E-VIGA	U-VIGA
CAT I	16			4		
CAT II	6.9	4.8	3.6	2	1.9	1.9
CAT III	4.1			2		

VI. CONCLUSIONS

The research activities performed to design a low-cost and low-weight/volume integrated Navigation and Guidance System (NGS) suitable for small size UA applications were described. Various sensors were considered for the design of the NGS including GNSS and MEMS-IMUs, with augmentation from ADM and VBN sensors. An innovative low-cost and low-weight/volume integrated Navigation and Guidance System (NGS) architecture was introduced based on an Unscented Kalman Filter (UKF). While the EKF based E-VIGA system uses unfiltered ADM data, the U-VIGA system employs an UKF for pre-filtering the ADM attitude solution, so to increase the ADM attitude solution stability (validity time of 65 sec before exceeding the RNP thresholds). Simulation of the E-VIGA integrated navigation mode showed that the proposed integration schemes can achieve the required horizontal/vertical position accuracies, with a significant improvement compared to stand-alone GNSS and integrated GNSS/INS. Compared to the E-VIGA system, the U-VIGA system showed an improvement of accuracy in the position and attitude measurements in addition to an increased ADM stability time. Furthermore, the integration schemes achieved horizontal/vertical position accuracies in line with CAT-II precision approach requirements. Current research activities are investigating novel Four Dimensional (4D) Trajectory Based Operations (TBO) system design for both manned and unmanned aircraft. Additionally, the application of alternative algorithms for multi-sensor data fusion and pre-processing of the ADM solution to further improve the validity time are being explored. Finally, integrity monitoring and augmentation functionalities for UA are being researched upon to improve the overall system performance. Based on preliminary results, it is anticipated that the multisensory integrated NGS will be significantly enhanced in terms of data, accuracy, continuity and integrity to fulfill present and likely future RNP requirements for a variety of UA mission- and safety-critical operational tasks.

REFERENCES

[1] CAA Safety Regulation Group, GPS integrity and potential impact on aviation safety, Paper 2003/09, Civil Aviation Authority, Cheltenham, UK, 2004.

[2] Degarmo, M. T., "Issues Concerning Integration of Unmanned Aerial Vehicles in Civil Airspace," The MITRE Corporation Center For Advanced Aviation System Development, 2004.

[3] Doc 9750 – Global Air Navigation Capacity & Efficiency Plan 2013-2028, The International Civil Aviation Organization (ICAO), 4th edition, Montreal, Canada, 2014.

[4] Federal Aviation Administration (FAA), AC 120-29A. Advisory Circular - Criteria for Approval of Category I and Category II Weather Minima for Approach, U.S. Department of Transportation, 2012.

[5] Gardi, A., Sabatini, R., Ramasamy, S., Kistan, T., "Real-Time Trajectory Optimisation Models for Next Generation Air Traffic Management Systems," Applied Mechanics and Materials, vol. 629, Trans Tech Publications, Switzerland, pp. 327-332, 2014. DOI: 10.4028/www.scientific.net/AMM.629.327

[6] Guoqiang, M., Drake, S., and Anderson, B. D., "Design of an Extended Kalman Filter for UAV Localization," IEEE Conference on Information, Decision and Control (IDC'07), Adelaide, Australia, 2007.

[7] Hannuksela, J., "Facial Feature Based Head Tracking and Pose Estimation," Department of Electrical and Information Engineering, University of Oulu, Finland, 2003.

[8] Hua, Y., and Welch, G., "Model-based 3D Object Tracking Using an Extended-extended Kalman Filter and Graphics Rendered Measurements," IEEE Computer Vision for Interactive and Intelligent Environment, Lexington, Kentucky, 2005.

[9] Ingemars, N., "A Feature based Face Tracker using Extended Kalman Filtering," Department of Electrical Engineering, Linköpings Universitet, Sweden, 2007.

[10] International Civil Aviation Organisation (ICAO), Doc 9750 for Global Air Navigation Plan for CNS/ATM Systems, 2nd edition, Montréal, Quebec, Canada, 2002.

[11] Doc 9613, Performance-based Navigation (PBN) Manual, The International Civil Aviation Organisation (ICAO), Montréal, Quebec, Canada, 2008.

[12] Aeronautical Telecommunications - Volume 1: Radio Navigation Aids, Annex 10 to the Convention on International Civil Aviation, The International Civil Aviation Organization (ICAO), 6th edition, Montreal, Quebec, Canada, 2006.

[13] Ling, K., Chow, D., Das, A., and Waslander, S. L., "Autonomous Maritime Landings for Low-Cost VTOL Aerial Vehicles," Canadian Conference on Computer and Robot Vision (CRV), Montréal, Quebec, pp. 32-39, 2014.

[14] Lozano, R., "Unmanned aerial vehicles: Embedded control," John Wiley & Sons, 2013.

[15] Lucieer A., Malenovský, Z., Veness, T., and Wallace, L., "HyperUAS—Imaging Spectroscopy from a Multirotor Unmanned Aircraft System," Journal of Field Robotics, vol. 31, pp. 571-590, 2014.

[16] Martin, T. L., and Campbell, D. A., "RPAS Integration Within an Australian ATM System: What Equipment and Which Airspace," 2014 International Conference in Unmanned Aircraft Systems (ICUAS), Orlando, Florida, USA, pp. 656-668, 2014.

[17] Mills, S., Pridmore, T., and Hills, M., "Tracking in a Hough Space with the Extended Kalman Filter," British Machine Vision Conference 2003 (BMVC 2003). doi:10.5244/C.17.18

[18] Mohammed, Y., Alzubaidi, A., "Extended Kalman Filter based Missile Tracking," International Journal of Computational Engineering Research (IJCER), ISSN (e): 2250 – 3005, vol. 04, issue 4, 2011.

[19] Myung, H., and Kanade, T., "Maneuver-based Autonomous Navigation of a Small Fixed-wing UAV," 2013 IEEE International Conference on Robotics and Automation (ICRA), pp. 3961-3968, 2013.

[20] Neculescu, D., Jassemi-Zargani, R., "Extended Kalman Filter-based Sensor Fusion for Operational Space Control of a Robot Arm," IEEE

Transactions on Instrumentation and Measurement, vol. 51, issue 6, pp. 1279-1282, 2002.

[21] Ong, H. T., "Tracking Anti-Ship Missiles Using Radar and Infra-Red Search and Track: Track Error Performance," No. DSTO-TR-1863, Defence Science and Technology Organisation (DSTO), Edinburgh, Australia, 2006.

[22] Pestana, J., Sanchez-Lopez, J. L., Saripalli, S., and Campoy, P., "Computer Vision Based General Object Following for GPS-Denied Multirotor Unmanned Vehicles," American Control Conference (ACC), pp. 1886-1891, 2014.

[23] Ramasamy, S., Sabatini, R., Gardi, A., Kistan, T., "Next Generation Flight Management System for Real-Time Trajectory Based Operations," Applied Mechanics and Materials, vol. 629, Trans Tech Publications, Switzerland, pp. 344-349, 2014. DOI: 10.4028/www.scientific.net/AMM.629.344

[24] Sabatini, R., Rodriguez, L., Kaharkar, A., Bartel, C., and Shaid, T., "Carrier-Phase GNSS Attitude Determination and Control System for Unmanned Aerial Vehicle Applications," ARPN Journal Of Systems And Software, ISSN: 2222-9833, vol. 2, no. 11, pp. 297-322, 2012.

[25] Sabatini, R., Cappello, F., Ramasamy, S., Gardi, A., and Clothier, R., "An Innovative Navigation and Guidance System for Small Unmanned Aircraft using Low-Cost Sensors," Journal of Aircraft Engineering and Aerospace Technology, 2014. (In press).

[26] Sabatini, R., Bartel, C., Kaharkar, A., Shaid, T., Rodriguez, L., Zammit-Mangion, D., et al., "Low-cost Navigation And Guidance Systems for Unmanned Aerial Vehicles. Part 1: Vision-based and Integrated Sensors," Annual of Navigation, vol. 19, issue 2, pp. 71-98, 2012.

[27] R., Ramasamy, S., Gardi, A. and Rodriguez, P., "Low-cost Sensors Data Fusion for Small Size Unmanned Aerial Vehicles Navigation and Guidance," International Journal of Unmanned Systems Engineering, vol. 1, issue 3, pp. 16-47, 2013. doi: 10.14323/ijuseng.2013.11

[28] Sabatini, R., Rodríguez, L., Kaharkar, A., Bartel, C. and Shaid, T., "Low-cost Vision Sensors and Integrated Systems for Unmanned Aerial Vehicle Navigation and Guidance," ARPN Journal of Systems and Software, ISSN: 2222-9833, vol. 2, issue 11, pp. 323-349, 2012.

[29] VanDyke, M. C., Schwartz, J. L., and Hall, C. D., "Unscented Kalman Filtering for Spacecraft Attitude State and Parameter Estimation," Department of Aerospace and Ocean Engineering, Virginia Polytechnic Institute & State University, Blacksburg, Virginia, USA, 2004.

[30] Zhao, Y., "GPS/IMU Integrated System for Land Vehicle Navigation based on MEMS," Licentiate Thesis, Division of Geodesy and Geoinfo.